

# Anomalies in $B$ -decays and $U(2)$ flavor symmetry

Riccardo Barbieri<sup>1,4</sup>, Gino Isidori<sup>2,3,a</sup>, Andrea Patteri<sup>2,5</sup>, Fabrizio Senia<sup>4</sup>

<sup>1</sup> Institute of Theoretical Studies, ETH Zürich, 8092 Zurich, Switzerland

<sup>2</sup> Physik-Institut, Universität Zürich, 8057 Zurich, Switzerland

<sup>3</sup> INFN, Laboratori Nazionali di Frascati, 00044 Frascati, Italy

<sup>4</sup> Scuola Normale Superiore, INFN, Piazza dei Cavalieri 7, 56126 Pisa, Italy

<sup>5</sup> Dipartimento di Fisica e Astronomia ‘G. Galilei’, Università di Padova, Via Marzolo 8, 35131 Padua, Italy

Received: 18 December 2015 / Accepted: 20 January 2016 / Published online: 8 February 2016

© The Author(s) 2016. This article is published with open access at Springerlink.com

**Abstract** The collection of a few anomalies in semileptonic  $B$ -decays invites to speculate about the emergence of some strikingly new phenomena. Here we offer a possible interpretation of these anomalies in the context of a weakly broken  $U(2)^5$  flavor symmetry and leptoquark mediators.

## 1 Introduction

In the last years quite a few anomalies in semileptonic  $B$ -decays have emerged. While individually any of them requires confirmation before being taken under serious consideration, their collection motivates to speculate about the possible emergence of some strikingly new phenomena. The purpose of this paper is to offer a possible interpretation of these anomalies in the context of a weakly broken  $U(2)^n$ -flavor symmetry.

The observations we refer to have received and are receiving a lot of attention. The deviations from the SM that are both statistically more significant and whose theoretical error is negligible (compared to the present experimental error) can be summarized as follows:

- An overall  $3.9\sigma$  deviation from  $\tau/l$  universality ( $l = \mu, e$ ) in charged-current semileptonic  $B \rightarrow D^{(*)}$  decays [1–3]:<sup>1</sup>

$$R_{D^{(*)}}^{\tau/l} = \frac{\mathcal{B}(\bar{B} \rightarrow D^{(*)}\tau\bar{\nu})/\mathcal{B}(\bar{B} \rightarrow D^{(*)}\tau\bar{\nu})_{SM}}{\mathcal{B}(\bar{B} \rightarrow D^{(*)}l\bar{\nu})/\mathcal{B}(\bar{B} \rightarrow D^{(*)}l\bar{\nu})_{SM}}, \quad (1.1)$$

$$R_D^{\tau/l} = 1.37 \pm 0.17, \quad R_{D^*}^{\tau/l} = 1.28 \pm 0.08 \quad (1.2)$$

<sup>1</sup> The results in Eq. (1.2) are obtained using the theory predictions  $\mathcal{B}(B \rightarrow D^*\tau\nu)/\mathcal{B}(B \rightarrow D^*l\nu)_{SM} = 0.252 \pm 0.003$  [5] and  $\mathcal{B}(B \rightarrow D\tau\nu)/\mathcal{B}(B \rightarrow Dl\nu)_{SM} = 0.300 \pm 0.008$  [6].

<sup>a</sup>e-mail: gino.isidori@lnf.infn.it

- A  $2.6\sigma$  deviation from  $\mu/e$  universality in the neutral-current  $b \rightarrow s$  transition [4]:

$$R_K^{\mu/e} = \frac{\mathcal{B}(B \rightarrow K\mu^+\mu^-)}{\mathcal{B}(B \rightarrow Ke^+e^-)} = 0.745_{-0.074}^{+0.090} \pm 0.036 \quad (1.3)$$

predicted to be one in the Standard Model (SM) with better than 1 % accuracy.

This last neutral-current anomaly may be related to other tensions with the SM in the branching ratios and in the angular distributions of semileptonic  $b \rightarrow s$  transitions, particularly in  $B \rightarrow K^{(*)}\mu^+\mu^-$  and  $B \rightarrow \phi\mu^+\mu^-$  (see Refs. [7,8] for an updated discussion).

The interpretation of a 30 % deviation from the SM in a tree-level charged-current interaction, Eq. (1.2), calls for an exchange capable to produce at low energy an effective 4-fermion interaction proportional to the operator  $(\bar{c}_L\gamma_\mu b_L)(\bar{\tau}_L\gamma_\mu\nu_L)$ . On these grounds one may want to interpret the neutral-current anomaly in Eq. (1.3) as also due to an LL operator of the form  $(\bar{s}_L\gamma_\mu b_L)(\bar{\mu}_L\gamma_\mu\mu_L)$ . Although not exclusively, it is known that such an operator can as well improve the fit in the angular distribution of the semileptonic  $b \rightarrow s$  transitions [7,8]. There is, however, a problem to face. While both anomalies hint at a 20 ÷ 30 % deviation from the SM, there is an important difference among them. The charged-current anomaly is a deviation from a SM tree-level amplitude involving the third generation of leptons, whereas the neutral-current one is a putative correction to a SM-loop effect only concerning the first two generations of leptons.

This motivates us to ask whether there is a flavor group  $\mathcal{G}_F$  and a tree-level exchange  $\Phi$  such that:

- With unbroken  $\mathcal{G}_F$ ,  $\Phi$  couples to the third generation of quarks and leptons only;

- After  $\mathcal{G}_F$ -breaking, the needed operators, as mentioned in the previous paragraph, are generated as a small perturbation.

The answer is positive with

$$\mathcal{G}_F = \mathcal{G}_F^q \times \mathcal{G}_F^l \tag{1.4}$$

$$\begin{aligned} \mathcal{G}_F^q &= U(2)_Q \times U(2)_u \times U(2)_d \times U(1)_{d3}, \\ \mathcal{G}_F^l &= U(2)_L \times U(2)_e \times U(1)_{e3}, \end{aligned} \tag{1.5}$$

in the notation of Refs. [9–12], and  $\Phi$  is a leptoquark singlet under  $\mathcal{G}_F$ , carrying either one of the following quantum numbers under the SM gauge group:

1.  $U_\mu = (3, 1)_{2/3}$ , vector-singlet model;
2.  $\mathcal{U}_\mu = (3, 3)_{2/3}$ , vector triplet model;
3.  $S = (\bar{3}, 3)_{1/3}$ , scalar triplet model.

Dynamical explanations of the above anomalies have already been proposed in the literature both in terms of vector uncolored mediators [13] and in terms of leptoquark mediators [14–16].<sup>2</sup> Here we focus on the specific realization of leptoquark models based on the flavor group  $\mathcal{G}_F$  since:

- (i) this explains their dominant coupling to the third generation only (in particular only to the left-handed quark and lepton doublets which are the only  $\mathcal{G}_F$ -invariant fermions);
- (ii) the breaking of  $\mathcal{G}_F$  specifies the source of the flavor violating couplings needed to give rise predominantly to the operator  $(\bar{c}_L \gamma_\mu b_L)(\bar{\tau}_L \gamma_\mu \nu_L)$  and, at a weaker level, to  $(\bar{s}_L \gamma_\mu b_L)(\bar{\mu}_L \gamma_\mu \mu_L)$  as well.

About the needed breakings of  $\mathcal{G}_F$ , we stick to the minimal set of spurions

$$\begin{aligned} y_{d3} &= (1, 1, 1)_{-1} \Delta_u = (2, \bar{2}, 1)_0 \Delta_d \\ &= (2, 1, \bar{2})_0 \mathbf{V}_Q = (2, 1, 1)_0 \end{aligned} \tag{1.6}$$

for  $\mathcal{G}_F^q$  [9] and

$$y_{e3} = (1, 1)_{-1} \quad \Delta_e = (2, \bar{2})_0 \quad \mathbf{V}_L = (2, 1)_0 \tag{1.7}$$

for  $\mathcal{G}_F^l$  [25, 26].

In the following we write down in the three cases above the leptoquark (LQ) couplings to the fermions in their physical bases after inclusion of  $\mathcal{G}_F$ -breaking (Sect. 2) and we calculate the relevant amplitudes at tree level (Sect. 3). Consistency with current data is achieved only by the  $U_\mu = (3, 1)_{2/3}$  model above. The dominant loop effects when the tree-level

amplitude vanishes are calculated in Sect. 4 for the surviving vector-singlet model. The overall consistency of the model with data is illustrated in Sect. 5, where further expected signals are also examined. A tentative UV completion of the phenomenological model is briefly outlined in Sect. 6. Summary and conclusions are drawn in Sect. 7.

## 2 Leptoquark Lagrangians after $\mathcal{G}_F$ -symmetry breaking

The couplings of the three LQ to the SM electroweak doublets  $Q_L$  and  $L_L$  are ( $a$  is an index in the vector representation of  $SU(2)_L$ , whereas the color indices are left understood)

$$\mathcal{L}_1 = g_U (\bar{Q}_L \gamma^\mu F L_L) U_\mu + \text{h.c.} \tag{2.1}$$

$$\mathcal{L}_2 = g_U \left( \bar{Q}_L \gamma^\mu \frac{\sigma^a}{2} F L_L \right) U_\mu^a + \text{h.c.} \tag{2.2}$$

$$\mathcal{L}_3 = g_S \left( \bar{Q}_L^c \frac{\sigma^a}{2} F (i\sigma^2 L_L) \right) S^a + \text{h.c.}; \quad Q_L^c \equiv (Q_L)^c \tag{2.3}$$

where  $F$  is a matrix in flavor space which, in the  $\mathcal{G}_F$  symmetric limit, is  $F_{ij} = \delta_{i3} \delta_{j3}$ . On the other hand, after symmetry breaking along the directions (1.6) and (1.7),  $F$  takes the form

$$F_{ij} = \delta_{i3} \delta_{j3} + a V_{Q_i} \delta_{j3} + b \delta_{i3} V_{L_j} + c V_{Q_i} V_{L_j} \tag{2.4}$$

where, by symmetry transformations, we can write

$$V_Q = \begin{pmatrix} 0 \\ \epsilon_Q \\ 0 \end{pmatrix} \quad V_L = \begin{pmatrix} 0 \\ \epsilon_L \\ 0 \end{pmatrix} \tag{2.5}$$

in terms of two small real parameters  $\epsilon_Q, \epsilon_L$ , and  $a, b, c$  are arbitrary coefficients, generically of order unity, that we shall also take real for simplicity. In Eq. (2.4) we neglect terms proportional to the product  $y_b y_\tau$  of the bottom and  $\tau$  Yukawa couplings or to products of  $\Delta_{u,d,e}$ . At the same time and in the same bases as Eq. (2.4), the Yukawa matrices for the charged fermions take the form

$$\begin{aligned} Y_u &= \begin{pmatrix} \Delta_u & y_t \mathbf{V}_Q \\ 0 & y_t \end{pmatrix} & Y_d &= \begin{pmatrix} \Delta_d & y_b x_b \mathbf{V}_Q \\ 0 & y_b \end{pmatrix} \\ Y_e &= \begin{pmatrix} \Delta_e & y_\tau \mathbf{V}_L \\ 0 & y_\tau \end{pmatrix} \end{aligned}$$

where  $x_b$  is another unknown coefficient in general of order unity.

One goes to the physical bases for all the charged fermions by an approximate diagonalization of these Yukawa matrices. In these physical bases the LQ interaction Lagrangians acquire the form

$$\mathcal{L}_1 = g_U (\bar{u}_L \gamma^\mu F^U \nu_L + \bar{d}_L \gamma^\mu F^D e_L) U_\mu + \text{h.c.} \tag{2.6}$$

<sup>2</sup> Leptoquark explanations of a single set of anomalies (either neutral or charged currents) have been discussed in Refs. [17–22]. For a recent discussion of the two set of anomalies in terms of effective four-fermion operators see Refs. [23, 24].

$$\begin{aligned} \mathcal{L}_2 = & \frac{g_U}{\sqrt{2}} \left[ \frac{1}{\sqrt{2}} (\bar{u}_L \gamma^\mu F^U \nu_L - \bar{d}_L \gamma^\mu F^D e_L) U_\mu^{2/3} \right. \\ & \left. + (\bar{u}_L \gamma^\mu F^U e_L) U_\mu^{5/3} + (\bar{d}_L \gamma^\mu F^D \nu_L) U_\mu^{-1/3} \right] \\ & + \text{h.c} \end{aligned} \tag{2.7}$$

$$\begin{aligned} \mathcal{L}_3 = & \frac{g_S}{\sqrt{2}} \left[ \frac{1}{\sqrt{2}} (\bar{u}_L^c F^U e_L + \bar{d}_L^c F^D \nu_L) S^{1/3} \right. \\ & \left. + (\bar{u}_L^c F^U \nu_L) S^{-2/3} + (\bar{d}_L^c F^D e_L) S^{4/3} \right] + \text{h.c} \end{aligned} \tag{2.8}$$

where

$$\begin{aligned} F^U = & \begin{pmatrix} V_{ub}(s_l \epsilon_l) A_u & V_{ub}(c_l \epsilon_l) A_u & V_{ub}(1-a)r_u \\ V_{cb}(s_l \epsilon_l) A_u & V_{cb}(c_l \epsilon_l) A_u & V_{cb}(1-a)r_u \\ V_{tb}(s_l \epsilon_l)(b-1) & V_{tb}(c_l \epsilon_l)(b-1) & V_{tb} \end{pmatrix} \tag{2.9} \\ F^D = & \begin{pmatrix} V_{td}(s_l \epsilon_l) A_d & V_{td}(c_l \epsilon_l) A_d & V_{td}[1-(1-a)r_u] \\ V_{ts}(s_l \epsilon_l) A_d & V_{ts}(c_l \epsilon_l) A_d & V_{ts}[1-(1-a)r_u] \\ V_{tb}(s_l \epsilon_l)(b-1) & V_{tb}(c_l \epsilon_l)(b-1) & V_{tb} \end{pmatrix} \end{aligned} \tag{2.10}$$

$$r_u = \frac{1}{1-x_b}, \quad A_u = r_u(b-1+a-c) \quad A_d = b-1-A_u, \tag{2.11}$$

and  $\theta_l$  is the angle ( $s_l = \sin \theta_l, c_l = \cos \theta_l$ ) in the unitary transformation that diagonalizes  $\Delta_l$  on the left side. We are working in the basis of neutrino current eigenstates, where the charged-current leptonic weak interactions are flavor-diagonal. We are also neglecting a phase in the 13 and 31 elements of these flavor matrices since it does not play any role in the following considerations.

### 3 Tree-level amplitudes

In the three models defined in Sect. 1 the tree-level exchanges of the corresponding LQ give rise to effective Lagrangians relevant to charged-current and neutral-current semileptonic  $B$  and  $K$  decays. For  $b \rightarrow c \tau \bar{\nu}_3$  one has

$$\begin{aligned} \mathcal{L}_{\text{eff}}^{b \rightarrow c \tau \nu} = & \left( -\frac{g_U^2}{M_U^2}, \frac{g_U^2}{4M_U^2}, \frac{g_S^2}{8M_S^2} \right) r_u \\ & \times V_{cb}(1-a) (\bar{c}_L \gamma_\mu b_L) (\bar{\tau}_L \gamma_\mu \nu_{3L}) \end{aligned} \tag{3.1}$$

to be compared with the SM result

$$\mathcal{L}_{SM}^{b \rightarrow c \tau \nu} = -\frac{g^2}{2M_W^2} V_{cb} (\bar{c}_L \gamma_\mu b_L) (\bar{\tau}_L \gamma_\mu \nu_{3L}). \tag{3.2}$$

In both cases (SM and LQ exchange) the  $b \rightarrow u \tau \bar{\nu}_3$  effective Lagrangians are obtained from the above ones with the exchange  $c \rightarrow u$  and  $V_{cb} \rightarrow V_{ub}$ .

For the neutral-current processes  $b \rightarrow s \ell \bar{\ell}$ , with  $\ell = e, \mu, \tau$ , the LQ exchange gives

$$\begin{aligned} \mathcal{L}_{\text{eff}}^{b \rightarrow s \mu \mu} = & \left( -\frac{g_U^2}{M_U^2}, -\frac{g_U^2}{4M_U^2}, \frac{g_S^2}{4M_S^2} \right) V_{tb} V_{ts}^* (\bar{s}_L \gamma_\mu b_L) \\ & \times [(1-(1-a)r_u) (\bar{\tau}_L \gamma_\mu \tau_L) \\ & + (c_l \epsilon_l)^2 (b-1) A_d (\bar{\mu}_L \gamma_\mu \mu_L) \\ & + (s_l \epsilon_l)^2 (b-1) A_d (\bar{e}_L \gamma_\mu e_L)], \end{aligned} \tag{3.3}$$

whereas the lepton-universal local  $b \rightarrow s \ell \bar{\ell}$  effective interaction present in the SM reads

$$\mathcal{L}_{SM}^{b \rightarrow s \ell \ell} \approx -\frac{8G_F}{\sqrt{2}} V_{tb} V_{ts}^* \frac{\alpha}{4\pi} C_9^{SM} (\bar{s}_L \gamma_\mu b_L) (\bar{\ell}_L \gamma_\mu \ell_L), \tag{3.4}$$

with  $C_9^{SM} \approx 4.2$ . Finally, for  $b \rightarrow s \nu_3 \bar{\nu}_3$  and  $s \rightarrow d \nu_3 \bar{\nu}_3$  amplitudes, the LQ exchange gives

$$\begin{aligned} \mathcal{L}_{\text{eff}}^{b(s) \rightarrow s(d) \nu \nu} = & \left( 0, -\frac{g_U^2}{2M_U^2}, \frac{g_S^2}{8M_S^2} \right) (\bar{\nu}_3 \gamma_\mu \nu_{3L}) \\ & \times [V_{tb} V_{ts}^* ((1+r_u(a-1)) (\bar{s}_L \gamma_\mu b_L) \\ & + V_{ts} V_{td}^* |1+r_u(a-1)|^2 (\bar{d}_L \gamma_\mu s_L)], \end{aligned} \tag{3.5}$$

to be compared with

$$\begin{aligned} \mathcal{L}_{SM}^{b(s) \rightarrow s(d) \nu \nu} = & -\frac{8G_F}{\sqrt{2}} C_v^{SM} \frac{\alpha}{4\pi} \\ & \times [V_{tb} V_{ts}^* (\bar{s}_L \gamma_\mu b_L) + V_{ts} V_{td}^* (\bar{d}_L \gamma_\mu s_L)] \\ & \times \sum_{i=1}^3 (\bar{\nu}_i \gamma_\mu \nu_{iL}), \end{aligned} \tag{3.6}$$

where  $C_v^{SM} \approx -6.3$  (and we have omitted the subleading charm contribution in the  $s \rightarrow d \nu \bar{\nu}$  case). Note the absence of a tree-level contribution to  $b \rightarrow s \nu \bar{\nu}$  from the  $SU(2)$ -singlet vector LQ (model 1), as noted first in Ref. [14].

#### 3.1 Tree-level constraints on the parameter spaces

From Eqs. (3.1) and (3.2), neglecting small corrections to  $\mathcal{B}(\bar{B} \rightarrow D^{(*)} l \bar{\nu})$  suppressed by the  $\epsilon_l$  factor, one has for the three models of Sect. 1

$$R_{D^{(*)}}^{\tau/l} \approx 1 + \left( R_U, -\frac{1}{4} R_U, -\frac{1}{8} R_S \right) r_u (1-a) \tag{3.7}$$

where

$$(R_U, R_U, R_S) = \frac{4M_W^2}{g^2} \left( \frac{g_U^2}{M_U^2}, \frac{g_U^2}{M_U^2}, \frac{g_S^2}{M_S^2} \right). \tag{3.8}$$

Similarly from Eqs. (3.5) and (3.6) one has

$$R_{K^{(*)}\nu} = \frac{\mathcal{B}(\bar{B} \rightarrow K^{(*)} \nu \bar{\nu})}{\mathcal{B}(\bar{B} \rightarrow K^{(*)} \nu \bar{\nu})_{SM}} \approx \frac{1}{3} (3 + 2\text{Re}(x) + |x|^2) \tag{3.9}$$

where for the various models it is

$$(x_U, x_U, x_S) = -\frac{\pi}{\alpha C_9^{SM}} [1 - r_u(1 - a)] \left(0, -\frac{R_U}{2}, \frac{R_S}{8}\right). \tag{3.10}$$

A similar formula holds for  $R_{\pi\nu\bar{\nu}} = \mathcal{B}(K \rightarrow \pi\nu\bar{\nu})/\mathcal{B}(K \rightarrow \pi\nu\bar{\nu})_{SM}$ , in the limit where we neglect the subleading charm contribution and replace  $[1 - r_u(1 - a)]$  with  $[1 - r_u(1 - a)]^2$ .

Unlike the case for  $\mathcal{L}_{\text{eff}}^{b \rightarrow s\mu\mu}$ , both  $R_{D^{(*)}}^{\tau/l}$  and  $R_{K^{(*)}\nu}$  depend on a single combination of flavor parameters  $\beta = 1 - r_u(1 - a)$ . This puts a strong constraint on models 2 and 3 of Sect. 1, shown in Fig. 1 (for  $R_{K^{(*)}\nu}$  we use the bound  $R_{K^{(*)}\nu} < 4.3$  [27]), making them highly disfavored [14]. From now on we therefore concentrate our attention on model 1 with a vector-singlet LQ.

For later use,  $R_K^{\mu/e}$  in this model is

$$R_K^{\mu/e} = \frac{\mathcal{B}(B \rightarrow K\mu^+\mu^-)}{\mathcal{B}(B \rightarrow Ke^+e^-)}$$

$$s = 1 + \left(\frac{2\pi}{\alpha C_9^{SM}}\right) [(b - 1)A_d] R_U \epsilon_l^2 (1 - 2s_l^2), \tag{3.11}$$

while the corresponding  $\tau/e$  and  $\tau/\mu$  ratios are

$$R_K^{\tau/e} \approx R_K^{\tau/\mu} \approx \left| 1 + \left(\frac{\pi}{\alpha C_9^{SM}}\right) [1 - (1 - a)r_u] R_U \right|^2$$

$$\approx 10^2 \times |1 - (1 - a)r_u|^2 \times \left(\frac{R_U}{0.1}\right)^2. \tag{3.12}$$

The result in Eq. (3.12) holds for any  $b \rightarrow s\tau\bar{\tau}$  rate, e.g. also for  $\mathcal{B}(B \rightarrow \tau^+\tau^-)$  and  $\mathcal{B}(B \rightarrow K^*\tau^+\tau^-)$ , normalized to its corresponding SM value. At present this does not represent a significant constraint given that the experimental upper bounds on these modes are still 3 orders of magnitude above the SM level [27], but in the future this large enhancement could provide a striking low-energy signature of the model.

To conclude this section, it is worth comparing the tree-level effects induced by the LQ exchange (model 1) with those analyzed in Ref. [13] assuming a vector uncolored mediator. The structure of the semileptonic operators generated is the same, but the relative weight of charged- and neutral-current terms is different: in Ref. [13] the neutral-current operators receive an additional overall suppression factor. This is why in Ref. [13] the non-standard effects are much smaller in the case of  $b \rightarrow s\nu\bar{\nu}$  and  $b \rightarrow s\tau\bar{\tau}$  transitions. Another difference is the absence, at the tree level, of LQ contributions to  $B$ -meson mixing. However, as we will discuss next, this difference is only apparent: quadratically divergent contributions to  $\Delta F = 2$  amplitudes are generated in the LQ case at the one-loop level and, similarly to the case of Ref. [13],  $B$ -meson mixing represents a significant constraint on the model.

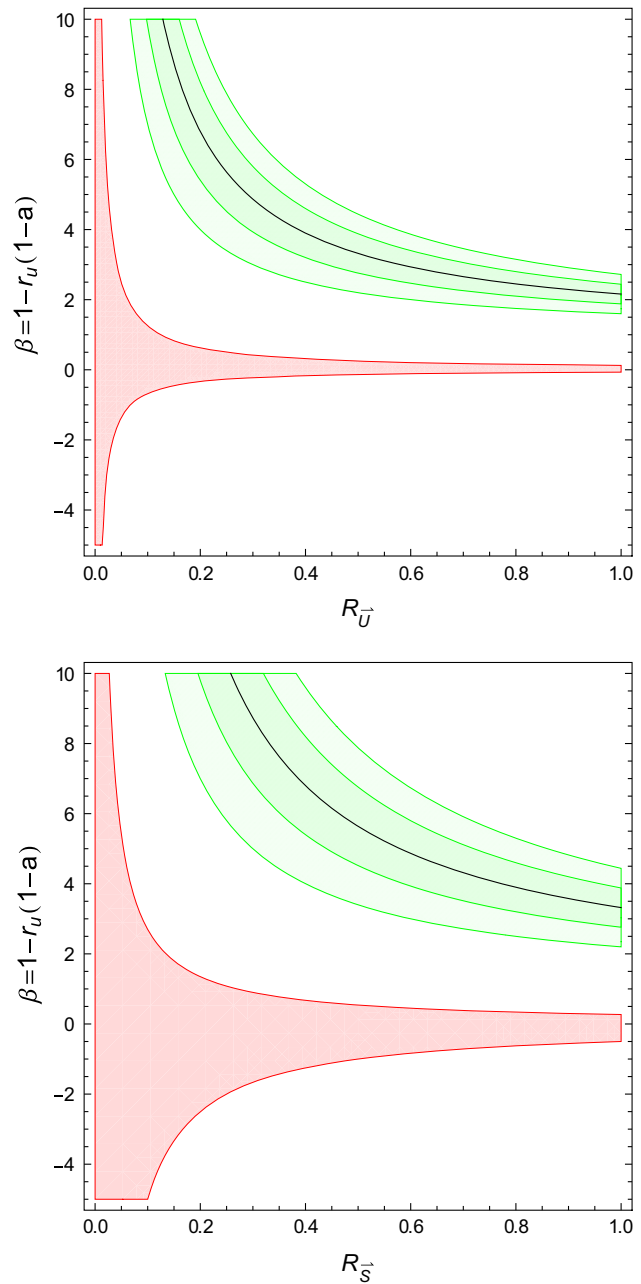


**Fig. 1** Allowed parameter spaces for the vector-triplet  $\mathbf{U}$  ( $up R_U = 4g_U^2 M_W^2 / g^2 M_U^2$ ) and for the scalar-triplet  $\mathbf{S}$  (down  $R_S = 4g_S^2 M_W^2 / g^2 M_S^2$ ) from  $R_{D^{(*)}}^{\tau/l}$  [at  $1\sigma$  ( $2\sigma$ ) darker (lighter) green region] and  $R_{K^{(*)}\nu}$  (red region)

### 4 Loop effects

Several processes exist which do not take place in the leptoquark models under consideration at tree level, but appear only at the one-loop level. A relevant example, as already noticed, is the  $b \rightarrow s\nu\bar{\nu}$  amplitude in the  $SU(2)$ -singlet vector leptoquark model 1 of Sect. 1. Since several of these processes can give significant constraints, a one-loop calcu-

lation is necessary, especially, but not only, when there are quadratically divergent contributions.

For the Lagrangian that describes the free propagation of the leptoquark  $U_\mu$  and its interactions with the SM gauge bosons we take

$$\mathcal{L}_U = -\frac{1}{2}U_{\mu\nu}^\dagger U^{\mu\nu} + M_U^2 U_\mu^\dagger U_\mu + \mathcal{L}_{an} \tag{4.1}$$

where

$$U_{\mu\nu} = D_\nu U_\mu - D_\nu U_\mu$$

$$D_\mu \equiv \partial_\mu - i g_s \frac{\lambda^a}{2} G_\mu^a - i g' \frac{2}{3} B_\mu \tag{4.2}$$

and

$$\mathcal{L}_{an} = -i g_s k_s \left( U_\mu^\dagger \frac{\lambda^a}{2} U_\nu \right) G^{\mu\nu a} - i g' \frac{2}{3} k_Y U_\mu^\dagger U_\nu B^{\mu\nu} \tag{4.3}$$

with obvious meaning of the symbols.  $\mathcal{L}_U$  is gauge invariant under the SM group for any value of  $k_s$  and  $k_Y$ . The overall interaction Lagrangian of the leptoquark with the  $B_\mu$  field is therefore

$$\mathcal{L}_{UUB} = i g' \frac{2}{3} \left[ (\partial_\alpha U_\beta^\dagger - \partial_\beta U_\alpha^\dagger) B^\alpha U^\beta - (\partial_\alpha U_\beta - \partial_\beta U_\alpha) B^\alpha U^{\beta+} - k_Y U_\mu^\dagger U_\nu \partial_\mu B_\nu + k_Y U_\mu U_\nu^\dagger \partial_\mu B_\nu \right]. \tag{4.4}$$

As a non-trivial check of our calculations it will be useful to notice that, for  $k_Y = 1$  and  $2/3 g' = g$ , Eq. (4.4) becomes the triple vertex among the  $W$  bosons in the SM with the identifications

$$B_\mu \rightarrow W_{3\mu}, \quad U_\mu \rightarrow W_\mu^+, \quad U_\mu^+ \rightarrow W_\mu^- \tag{4.5}$$

for a fixed color component of the leptoquark field.

### 4.1 Quadratically divergent loop effects

From exchanges of the  $U_\mu$  vector quadratically divergent corrections appear: (i) in the 2-point function of the  $B_\mu$  field, (ii) in the 3-point function between  $B_\mu$  and the fermion fields, (iii) in box-diagram contributions to various 4-fermion interactions. Below we list the relevant corrections.

#### 4.1.1 Two and three-point functions

In the LQ model we have the following contribution to the  $B_\mu$  propagator:

$$\Pi_{\mu\nu}^{BB} = i g_{\mu\nu} \left[ -k_Y^2 \frac{(4/9)g'^2}{64\pi^2} \frac{q^4}{M_U^2} \frac{\Lambda^2}{M_U^2} \right]. \tag{4.6}$$

We do not include a correction to  $\Pi_{\mu\nu}^{BB}$  at  $q^2 = 0$ , which vanishes by electromagnetic gauge invariance, nor a contribution

proportional to  $q^2$  since it is reabsorbed in a redefinition of  $g'$ .

Similarly one has  $\Lambda^2$ -divergences in the 3-point correlation functions with an external  $B_\mu$  field

$$\mathcal{M}_{B \rightarrow L_3 \bar{L}_3} = -i 3 k_Y \frac{(2/3)g'}{64\pi^2} g_U^2 \frac{q^2}{M_U^2} \frac{\Lambda^2}{M_U^2} (\bar{u}_{L3} \not{\epsilon} P_L v_{L3}), \tag{4.7}$$

$$\mathcal{M}_{B \rightarrow Q_3 \bar{Q}_3} = i k_Y \frac{(2/3)g'}{64\pi^2} g_U^2 \frac{q^2}{M_U^2} \frac{\Lambda^2}{M_U^2} (\bar{u}_{Q3} \not{\epsilon} P_L v_{Q3}). \tag{4.8}$$

As remarked above, this implies the presence in the SM in the unitary gauge of similar contributions in the 2 and 3-point functions of the  $W_\mu^a$  field, at  $g' = 0$ ,

$$\Pi_{\mu\nu}^{ab} = i g_{\mu\nu} \delta^{ab} \left[ -\frac{g^2}{64\pi^2} \frac{q^4}{M_W^2} \frac{\Lambda^2}{M_W^2} \right] \tag{4.9}$$

and

$$\mathcal{M}_{W_a \rightarrow F \bar{F}} = i g \frac{g^2}{64\pi^2} \frac{q^2}{M_W^2} \frac{\Lambda^2}{M_W^2} (\bar{u}_F T^a \not{\epsilon} P_L v_F), \tag{4.10}$$

where  $F = Q$  or  $L$  and  $T^a$  is the weak isospin. We have explicitly checked that quadratically divergent contributions to physical amplitudes vanish in this limit of the SM, as they should, with the inclusion of box diagrams as well.

#### 4.1.2 Box diagrams

Some relevant flavor violating processes have  $\Lambda^2$ -divergent contributions due to leptoquark box diagrams as well. The corresponding effective Lagrangian has the form

$$\mathcal{L} = \sum_a F_a W_a \frac{g_U^4}{64\pi^2} \frac{\Lambda^2}{M_U^4} O_a \tag{4.11}$$

with the process-dependent effective operators and the corresponding coefficients ( $F_a W_a$ ) given in Table 1.

### 4.2 Dipole operators

Unlike the previous cases, the coefficients of the dipole operators are not quadratically divergent. Yet they are logarithmically divergent and yield potentially relevant constraints given the stringent experimental bounds on  $\tau \rightarrow \mu\gamma$ ,  $\mu \rightarrow e\gamma$  and  $b \rightarrow s\gamma$ . The leading LQ contributions to these processes are encoded by

$$\mathcal{L} = \sum_a F_a \frac{g_U^2}{32\pi^2 M_U^2} (1 - k_Y) \text{Log} \left( \frac{\Lambda^2}{M_U^2} \right) O_a \tag{4.12}$$



**Table 1** Flavor coefficients  $F_a \times W_a$  for the box-diagram contributions to the different processes. In the last column are the bounds from current data for  $\Lambda = 4\pi M_U/g_U$  (see Sect. 5.3). The experimental constraints on the various processes are taken from Ref. [27]

Process	Operator	$F_a$	$W_a$	Bounds on $F_a \times (R/0.1)$
$\tau \rightarrow 3\mu$	$(\bar{\mu}\gamma^\mu P_L \tau)(\bar{\mu}\gamma_\mu P_L \mu)$	$3(b-1)^3(c_l \epsilon_l)^3$	1	$1.9 \times 10^{-2}$
$\mu \rightarrow 3e$	$(\bar{e}\gamma^\mu P_L \mu)(\bar{e}\gamma_\mu P_L e)$	$3(b-1)^4(c_l \epsilon_l)(s_l \epsilon_l)^3$	1	$5.5 \times 10^{-5}$
$b \rightarrow s\nu_3\bar{\nu}_3$	$(\bar{s}\gamma^\mu P_L b)(\bar{\nu}_3\gamma_\mu P_L \nu_3)$	$[1 - (1-a)r_u]$	$V_{tb}V_{ts}^*$	$[-2.5, 1.4]$
$s \rightarrow d\nu_3\bar{\nu}_3$	$(\bar{d}\gamma^\mu P_L s)(\bar{\nu}_3\gamma_\mu P_L \nu_3)$	$[1 - (1-a)r_u]^2$	$V_{ts}V_{td}^*$	$[-1.8, 0.6]$
$b\bar{s} \rightarrow \bar{b}s$	$(\bar{s}\gamma^\mu P_L b)^2$	$[1 - (1-a)r_u]^2$	$(V_{tb}V_{ts}^*)^2$	$3.0 \times 10^{-2}$

where

$$O_{\tau\mu\gamma} = em_\tau(\bar{\mu}_L\sigma^{\alpha\beta}\tau_R)F_{\alpha\beta}, \quad F_{\tau\mu} = (b-1)(c_l\epsilon_l), \quad (4.13)$$

$$O_{\mu e\gamma} = em_\mu(\bar{e}_L\sigma^{\alpha\beta}\mu_R)F_{\alpha\beta}, \quad F_{\mu e} = (b-1)^2(c_l\epsilon_l)(s_l\epsilon_l), \quad (4.14)$$

$$O_{bs\gamma} = emb(\bar{s}_L\sigma^{\alpha\beta}b_R)F_{\alpha\beta}, \quad F_{bs} = \frac{1}{3}V_{tb}V_{ts}^*[1 - (1-a)r_u]. \quad (4.15)$$

### 5 Consistency with data and expected signals

#### 5.1 Electroweak precision tests

At the one-loop level in the leptoquark vector-singlet model there are no corrections to the  $S, T, U$  parameters. This is due to the fact that  $U_\mu$  only couples to  $B_\mu$  and not to the  $W_\mu^a$ -fields. There are, however, corrections to the electroweak Precision Tests (EWPT) due to higher dimensional operators, which are at least in principle important due to  $\Lambda^2$ -divergent effects.

The most effective way to see these effects is by considering the  $\epsilon_i$ -parameters, as defined in [28, 29], and their expressions in terms of vacuum-polarization, box-diagram, and vertex corrections for  $S, T, U = 0$  [30]. More specifically, in the limit where one neglects the small  $\mathcal{G}_F$ -breaking, the first two generations receive corrections only from  $\Pi_{\mu\nu}^{BB} = -ig_{\mu\nu}\Pi(q^2)$ :

$$\begin{aligned} \epsilon_1^{(1,2)} &= -e_5, & \epsilon_2^{(1,2)} &= -s^2e_4 - c^2e_5, \\ \epsilon_3^{(1,2)} &= c^2e_4 - c^2e_5, \end{aligned} \quad (5.1)$$

where

$$\begin{aligned} e_4^{(1,2)} &= -\frac{c^2}{2}\frac{d\Pi}{dq^2}(M_Z^2) = -c^2A, \\ e_5^{(1,2)} &= s^2\frac{M_Z^2}{2}\frac{d^2\Pi}{d(q^2)^2} = s^2A, \end{aligned} \quad (5.2)$$

and

$$\begin{aligned} A &= k_Y^2\frac{(4/9)g'^2}{64\pi^2}\frac{M_Z^2}{M_U^2}\frac{\Lambda^2}{M_U^2}, & c^2 &= 1 - \sin^2\theta_W, \\ \tan\theta_W &= \frac{g'}{g}. \end{aligned} \quad (5.3)$$

To estimate  $A$ , we take  $\Lambda \approx 4\pi M_U/g_U$ , which gives

$$A \approx \frac{k_Y^2}{36c^2}\left(\frac{gg'}{g_U^2}\right)^2 R_U. \quad (5.4)$$

Given the bounds on the deviations from the SM of the  $\epsilon_i$  at the  $10^{-3}$  level, with  $R_U \approx 0.1$  and  $g_U^2/(gg') \gtrsim 2 \div 3$ , this is a mild constraint on  $k_Y$ .

Still without any  $\mathcal{G}_F$ -breaking, a vertex correction intervenes in  $Z$ -decays to the third generation. Specifically, from Eq. (4.8), the corresponding amplitudes get corrected as

$$\begin{aligned} \delta A_\mu(Z \rightarrow \tau^+\tau^-) &= -i\frac{\delta g}{2}(\bar{u}\gamma_\mu P_L v), \\ \delta A_\mu(Z \rightarrow b\bar{b}) &= i\frac{\delta g}{6}(\bar{u}\gamma_\mu P_L v), \end{aligned} \quad (5.5)$$

where

$$\frac{\delta g}{g} = -4\frac{s^2}{c}k_Y\frac{g_U^2}{64\pi^2}\frac{M_Z^2}{M_U^2}\frac{\Lambda^2}{M_U^2}, \quad (5.6)$$

which can be estimated as

$$\left|\frac{\delta g}{g}\right| \approx s\frac{k_Y}{4c^2}\left(\frac{gg'}{g_U^2}\right)R_U. \quad (5.7)$$

Consistency with the few *per mille* measurement of  $\mathcal{B}(Z \rightarrow \tau^+\tau^-)$  and  $R_U \approx 0.2$  requires

$$k_Y \lesssim 3 \times 10^{-2}\frac{g_U^2}{gg'}. \quad (5.8)$$

#### 5.2 Box diagrams and dipole operators

Some of the box-diagram contributions shown in Table 1 give extra significant constraints on the parameter space of the leptoquark vector-singlet model. Such constraints are given in the last column of Table 1 on the modulus of the corresponding flavor coefficients, with the exception of  $b \rightarrow s\nu_3\bar{\nu}_3$  and  $s \rightarrow d\nu_3\bar{\nu}_3$ , where there is an allowed range. We neglect the contributions, when present, of quadratically divergent penguin-like contributions proportional to  $k_Y$ .

Although the coefficients of the dipole operators in Sect. 4.2 are not quadratically divergent, they are significant at least

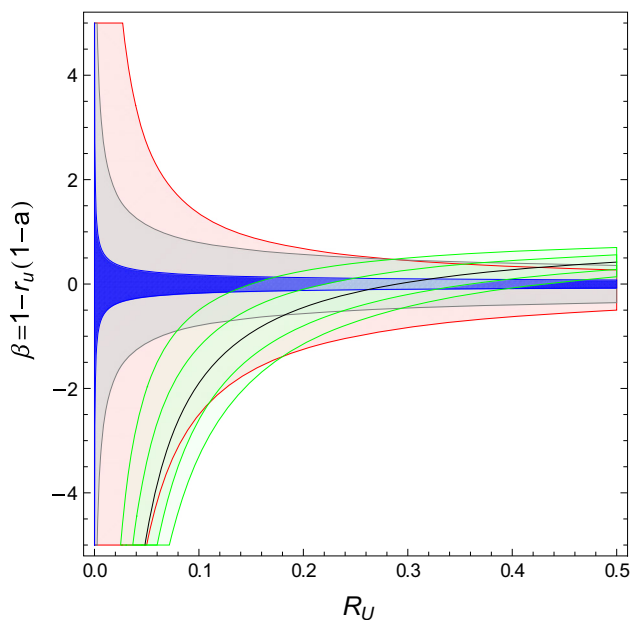


**Fig. 2** Allowed parameter space for the vector-singlet  $U$  from  $\Delta B_s = 2$  (blue region),  $R_{D^{τ/l}}^{(*)}$  (green),  $R_{K^{(*)ν}}$  (red) and  $\mathcal{B}(K^+ \rightarrow \pi^+ \nu \bar{\nu})$  (gray).  $R_U = 4g_U^2 M_W^2 / g^2 M_U^2$

in the leptonic processes. The bound on the flavor coefficient relevant to  $\tau \rightarrow \mu \gamma$  (obtained in the limit  $k_Y = 0$ ) is

$$(b - 1)(c_l \epsilon_l) \log(\Lambda / M_U) \lesssim 4 \times 10^{-2} \left(\frac{0.1}{R}\right), \quad (5.9)$$

whereas the one on  $\mu \rightarrow e \gamma$  is

$$(b - 1)^2 (s_l c_l) \epsilon_l^2 \log(\Lambda / M_U) \lesssim 5 \times 10^{-5} \left(\frac{0.1}{R}\right). \quad (5.10)$$

### 5.3 Overall constraints

As apparent from Sects. 3.1 and 5.2 the leptoquark effects in  $R_{D^{τ/l}}^{(*)}$  (at tree level),  $R_{K^{(*)ν}}$ ,  $\mathcal{B}(K^+ \rightarrow \pi^+ \nu \bar{\nu})$  and  $b\bar{s} \rightarrow \bar{b}s$  (at loop level) are predicted in terms of two single effective parameters,  $R_U$  and  $\beta = 1 - (1 - a)r_u$ , for a cutoff  $\Lambda \approx 4\pi M_U / g_U$ . The consistency with data of all these effects is shown in Fig. 2 for  $\Lambda = 4\pi M_U / g_U$ . The constraint from  $\Delta B_s = 2$  dominates over the others, fixing  $\beta$  near zero, within about  $0.1 \div 0.2$ . At the same time, at  $1\sigma$  level,  $R_U \approx 0.25 \div 0.35$ .

The leptoquark effects in  $R_K^{\mu/e}$  (at tree level) and in the purely leptonic sector (at loop level) depend, for given  $R_U$ , on  $\epsilon_l$  and  $s_l$  plus two combinations of parameters,  $(b - 1)$  and  $A_u = r_u(b - 1 + a - c)$ , generally of order unity. As shown more explicitly in a while, the dipole contribution to  $\mu \rightarrow e \gamma$  in Eq. (5.10) requires a small  $s_l$ . In this case the lepton flavor violating anomaly  $R_K^{\mu/e}$  constrains the parameter space as shown in Fig. 3, thus setting a lower bound on the combination  $[c_l \epsilon_l (b - 1)] \gtrsim 0.02$  for  $A_u / (b - 1) \lesssim 5$ .

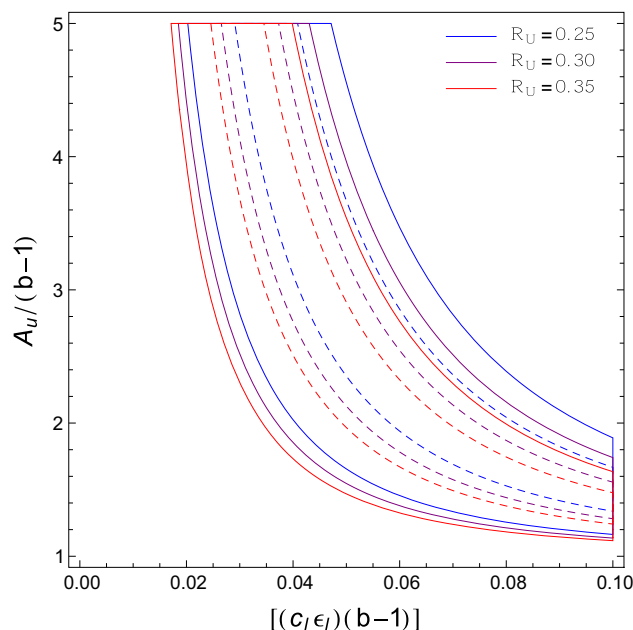


**Fig. 3** Allowed parameter space for the vector-singlet  $U$  from  $R_K^{\mu/e}$  for  $R_U = 0.25, 0.30, 0.35$ . Dotted (full) contours delimit the  $1\sigma$  ( $2\sigma$ ) regions

In turn the dipole contributions to  $\tau \rightarrow \mu \gamma$  and to  $\mu \rightarrow e \gamma$  (in this case for two values of  $s_l$ ) are shown in Fig. 4 against the same combination of parameters and different values of  $\Lambda / M_U$ . Both Figs. 3 and 4 are meant to be extended symmetrically for negative values of  $[c_l \epsilon_l (b - 1)]$ . Note that, for not too small values of  $s_l$ , it is  $\tau \rightarrow \mu \gamma$  that sets the strongest constraint. In fact, for  $A_u / (b - 1) \lesssim 5$ , all anomalies can be described consistently with all various constraints for values of  $\Lambda / M_U$  not larger than about  $3 \div 4$ , suggesting a strong interaction nature of the LQ.

### 5.4 Leptoquark pair production at LHC

The LQ production at the LHC is dominated by the QCD pair production and it depends only on  $M_U$ . A compilation of results relevant to our model 1 can be found, for instance, in the recent CMS analysis [31]: the cross-section varies from about 1 pb for  $M_U \approx 0.5$  TeV to  $3 \times 10^{-3}$  pb for  $M_U \approx 1.0$  TeV.<sup>3</sup>

In order to determine the LHC sensitivity to various LQ searches we need to evaluate the branching ratios in the different decay channels. At the tree level one has

$$\Gamma(U \rightarrow q_i \ell_j) = \frac{1}{24\pi} g_U^2 |F_{ij}^{U,D}|^2 M_U \quad (5.11)$$

and, to a good accuracy, the total decay width is given by the sum of the two leading decays ( $U \rightarrow t \bar{\nu}_\tau, b \bar{\tau}$ ):  $\Gamma_{\text{tot}} = g_U^2 M_U / (12\pi)$ . The branching ratios are then just given by

<sup>3</sup> By taking  $k_s = 0$  in Eq. (4.3).

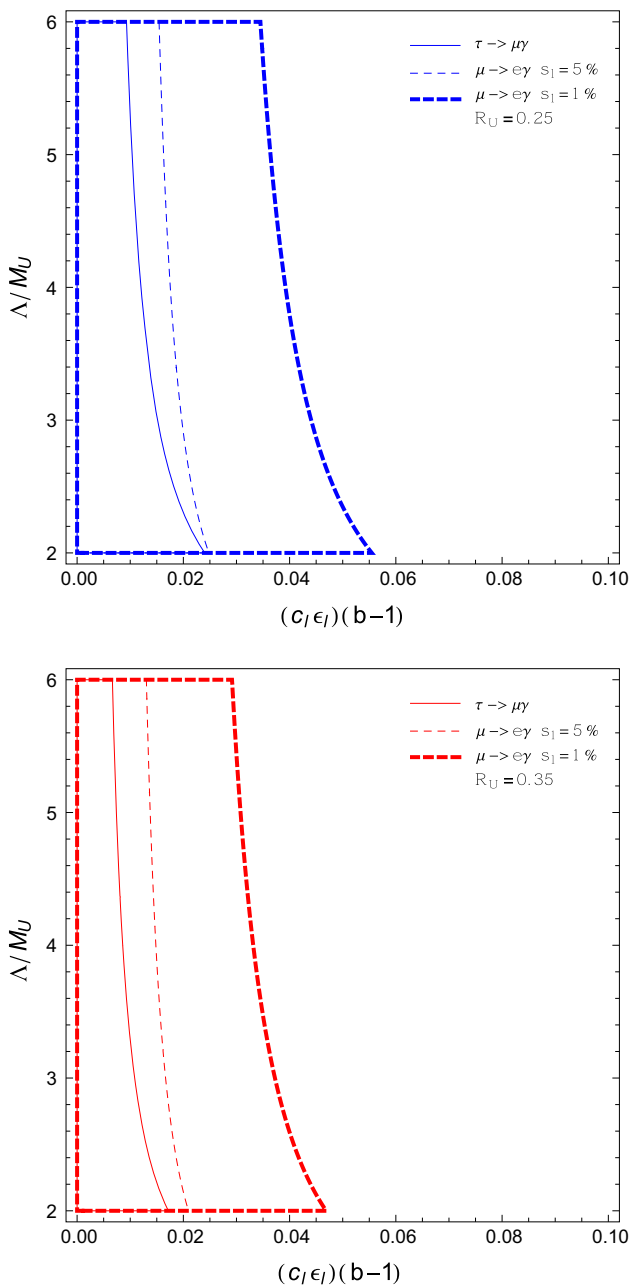


**Fig. 4** Allowed parameter space for the vector-singlet  $U$  from  $\tau \rightarrow \mu\gamma$  and  $\mu \rightarrow e\gamma$  for  $R_U = 0.25$  (up) and  $R_U = 0.35$  (down)

$$\begin{aligned} \mathcal{B}(U \rightarrow u_i \bar{\nu}_j) &= \frac{1}{2} |F_{ij}^U|^2, \\ \mathcal{B}(U \rightarrow d_i \ell_j^+) &= \frac{1}{2} |F_{ij}^D|^2. \end{aligned} \tag{5.12}$$

For the searches in the second-generation channels performed in Ref. [31] ( $U\bar{U} \rightarrow \mu\mu jj$  and  $U\bar{U} \rightarrow \mu\nu jj$ , where  $j$  denotes a light-quark jet) we find

$$\begin{aligned} \mathcal{B}(U\bar{U} \rightarrow \mu\mu jj) &= \left( \frac{1}{2} \sum_{i=d,s} |F_{i2}^D|^2 \right)^2 \approx (8.5 \times 10^{-7}) \times c_l^4 \epsilon_l^4, \end{aligned}$$

$$\begin{aligned} \mathcal{B}(U\bar{U} \rightarrow \mu\nu jj) &= \frac{1}{2} \sum_{i=d,s} |F_{i2}^D|^2 \frac{1}{2} \sum_{j=u,c} (|F_{j2}^U|^2 + |F_{j1}^U|^2) \\ &\approx (7.7 \times 10^{-7}) \times c_l^2 \epsilon_l^4, \end{aligned} \tag{5.13}$$

from which we deduce that these searches do not put any significant constraint on the model.

On the other hand, a relevant constraint is obtained by the dedicated search for the  $U\bar{U} \rightarrow t\bar{t}\nu_\tau\bar{\nu}_\tau$  decay chain performed by ATLAS [32]. In our model  $\mathcal{B}(U\bar{U} \rightarrow t\bar{t}\nu_\tau\bar{\nu}_\tau) = 0.25$  that implies the limit

$$M_U > 770 \text{ GeV}. \tag{5.14}$$

By a naive scaling of the statistics and the cross-section, we estimate that this limit could improve up to 1.3 TeV, in absence of a signal, with  $300 \text{ fb}^{-1}$  at 13 TeV.

Taking into account the constraints on  $R_U$  in Fig. 2, the bound on  $M_U$  can be turned into a bound on  $g_U$ . For  $R_U > 0.2$  we get  $g_U > 1.4$ , which would increase to  $g_U > 2.4$  in the absence of a direct signal with  $300 \text{ fb}^{-1}$  at 13 TeV.

### 6 A naive composite leptoquark picture

Needless to say the phenomenological model described so far cries out for a UV completion. Here we describe an attempt in the direction of composite Higgs models that will at least serve to illustrate the difficulties to comply with the various constraints. It does not take much to anticipate that the main such constraint comes from the value of  $R_U$  as implied by Fig. 2.

Let us consider a strongly interaction sector with a global symmetry  $SU(4) \times SO(5)$  spontaneously broken down to the Pati–Salam group  $SU(4) \times SU(2)_L \times SU(2)_R$ , so as to generate a composite pseudo-Goldstone Higgs boson. As usual the SM group is gauged inside the residual global group. Within  $SU(4)$  this structure leads to composite quasi-degenerate vectors: the composite gluons, a vector singlet carrying  $B-L$  and, most importantly, the  $U_\mu$  leptoquark vector.

The strong sector will also contain composite vector-like fermions in multiplets of the Pati–Salam group occurring in three flavor species. The important thing is that these composite  $\Psi$  fermions have components that match the quantum numbers of the SM fermions with respect to the SM gauge group. The requisite to make contact with the phenomenological model described in the previous Sects. is that the mass mixing terms between the elementary and the composite fermions respect, up to small breaking terms, the symmetry in flavor space  $U(2)_\Psi \times \mathcal{G}_F$ .<sup>4</sup> With  $\Psi = (4, 2, 1) \oplus (\bar{4}, 1, 2)$  (plus complex conjugate states) it is easy to convince oneself

<sup>4</sup> If  $\Psi$  is reducible  $U(2)_\Psi$  may actually be a product of  $U(2)$  factors.



that this structure shall lead, in the unbroken  $U(2)_\Psi \times \mathcal{G}_F$  limit, to Eq. (2.1) with

$$g_U = g^* \sin \theta_{Q3} \sin \theta_{L3} \quad (6.1)$$

and  $F_{ij} = \delta_{i3} \delta_{j3}$  as the only interaction of  $U_\mu$  with the standard fermions. Here  $g^*$  is the coupling of the LQ to the composite fermions and  $\theta_{Q3}, \theta_{L3}$  are the mixing angles of  $Q_3, L_3$  with the same composite fermions in  $\Psi$ . Other choices of  $\Psi$ , phenomenologically motivated, shall lead to a relation between  $g_U$  and  $g^*$  involving more parameters but always respecting  $g_U \leq g^*$ .

The “standard” interpretation of the composite Higgs models also gives a similar mass  $M \approx g^* f$  for the composite vectors in the adjoint of  $SU(4)$ , among which is  $U_\mu$ , and  $f$  is the breaking scale of  $SO(5)$  down to  $SO(4)$ . As a consequence the phenomenological parameter  $R_U$  becomes

$$R_U \approx \left(\frac{V}{f}\right)^2 \sin^2 \theta_{Q3} \sin^2 \theta_{L3}, \quad V = 245 \text{ GeV}, \quad (6.2)$$

independent from  $g^*$ .

## 7 Summary and conclusions

Being the heaviest particle in the SM, the top quark plays a special role in many processes and/or mechanisms of the greatest relevance in particle physics. It is not surprising therefore that the top quark is thought to be equally important in several BSM speculative considerations. Flavor physics is no exception to this rule. In the SM top exchanges dominate many of the observed flavor changing neutral current effects. In BSM, taking minimal flavor violation as a relevant example, it is the relatively large top Yukawa coupling that controls many of the new observable phenomena that might occur.

This is the basis to consider a  $U(2)^3$  approximate symmetry as a ruling symmetry of the flavor quark sector of any putative extension of the SM. More precisely  $U(2)_Q \times U(2)_u \times U(2)_d \times U(1)_{d3}$ , a residual symmetry of the SM with all the Yukawa coupling switched off but the top one, can allow, suitably broken, for mild deviations from the SM itself. Decays of the  $B$  mesons, in particular through the  $b_L$ -component, which is the only singlet under  $U(2)^3 \times U(1)_{d3}$  other than  $t_{L,R}$ , are obvious candidates where such deviations might occur and be observable.

It is therefore natural to ask if and how the recently emerged anomalies in semileptonic  $B$ -decays can be accommodated in this context. As we have shown this is possible by:

- (i) invoking the exchange of a vector-singlet LQ with a relatively large value of the parameter  $R_U = 4M_W^2 g_U^2 / g^2 M_U^2 \approx 0.2$ , i.e. a ratio well below 1 TeV between its mass  $M_U$  and its dominant coupling  $g_U$  to the third generation of left-handed quarks and leptons;

- (ii) extending the  $U(2)^3 \times U(1)_{d3}$  symmetry of the quark sector, with its breaking, to the lepton sector as well, via a  $U(2)_L \times U(2)_e \times U(1)_{e3}$  flavor symmetry.

The observed anomalies arise as relatively small effects of the breaking of the overall  $U(2)^5$  symmetry, thus allowing non-vanishing couplings of the LQ to the lighter generations as well.

The deviation from the SM in the charged-current observable  $R_{D^{(*)}}^{\tau/l}$  is due to a tree-level exchange of the LQ controlled, other than by  $R_U$ , by a single combination of dimensionless parameters  $\beta$ , as shown in Fig. 2. The same effective parameter controls the quadratically divergent one-loop contributions to  $B \rightarrow K \nu_3 \bar{\nu}_3$ ,  $K \rightarrow \pi \nu_3 \bar{\nu}_3$  and  $b\bar{s} \rightarrow \bar{b}s$ , as well as the tree-level effect in  $b \rightarrow s \tau \bar{\tau}$ . All of these processes can corroborate or exclude the LQ model by future measurements.

The lepton flavor violation emerging in the neutral-current observable  $R_K^{\mu/e}$  can also arise from a tree-level exchange of the leptoquark, although suppressed by the intervention in the final state of muons or electrons. In this case the relevant parameters control as well the log-divergent one-loop dipole moment contributions to  $\tau \rightarrow \mu \gamma$  and  $\mu \rightarrow e \gamma$ . The current limits on both these processes are close to saturate the observed deviation of  $R_K^{\mu/e}$  from unity, at least in a natural range of the relevant parameters, as illustrated in Figs. 3 and 4.

To discuss the possible manifestation of the vector LQ in direct production strongly depends on being able to go beyond the low energy phenomenological picture that we have used in this paper. This is because the constraint on  $R_U \approx 0.2$  only fixes the ratio  $M_U/g_U$  between the mass and the coupling of the LQ. The current LHC searches bound  $M_U$  to be bigger than about 700 GeV, independently from the value of  $g_U$ , which is therefore constrained to be bigger than about 1.4. Larger values of  $g_U$ , and therefore of  $M_U$  as well, are indirectly hinted by the constraints from  $\tau \rightarrow \mu \gamma$  and  $\mu \rightarrow e \gamma$ . All this points toward the need of a UV completion of the phenomenological model used so far, perhaps along the lines outlined in Sect. 6. It will be interesting to see if and how such UV completion can be accomplished consistently with the numerous constraints.

**Acknowledgments** We thank Andrea Tesi and Andrea Wulzer for useful discussions. This research was supported in part by the Swiss National Science Foundation (SNF) under contract 200021-159720.

**Open Access** This article is distributed under the terms of the Creative Commons Attribution 4.0 International License (<http://creativecommons.org/licenses/by/4.0/>), which permits unrestricted use, distribution, and reproduction in any medium, provided you give appropriate credit to the original author(s) and the source, provide a link to the Creative Commons license, and indicate if changes were made. Funded by SCOAP<sup>3</sup>.

## References

1. J. P. Lees et al., [BaBar Collaboration], Phys. Rev. D **88**(7), 072012 (2013). [arXiv:1303.0571](#)
2. M. Huschle et al., [Belle Collaboration], Phys. Rev. D **92**(7), 072014 (2015). [arXiv:1507.03233](#)
3. R. Aaij et al., [LHCb Collaboration], Phys. Rev. Lett. **115**(15), 159901 (2015). [arXiv:1506.08614](#)
4. R. Aaij et al., LHCb Collaboration. Phys. Rev. Lett. **113**, 151601 (2014). [arXiv:1406.6482](#)
5. S. Fajfer, J.F. Kamenik, I. Nisandzic, Phys. Rev. D **85**, 094025 (2012). [arXiv:1203.2654](#)
6. H. Na et al., [HPQCD Collaboration], Phys. Rev. D **92**(5), 054510 (2015). [arXiv:1505.03925](#)
7. S. Descotes-Genon, L. Hofer, J. Matias, J. Virto, [arXiv:1510.04239](#)
8. W. Altmannshofer, D.M. Straub, Eur. Phys. J. C **75**(8), 382 (2015). [arXiv:1411.3161](#)
9. R. Barbieri, G. Isidori, J. Jones-Perez, P. Lodone, D.M. Straub, Eur. Phys. J. C **71**, 1725 (2011). [arXiv:1105.2296](#)
10. R.S. Chivukula, H. Georgi, Phys. Lett. B **188**, 99 (1987)
11. L.J. Hall, L. Randall, Phys. Rev. Lett. **65**, 2939 (1990)
12. G. D'Ambrosio, G.F. Giudice, G. Isidori, A. Strumia, Nucl. Phys. B **645**, 155 (2002). [arXiv:hep-ph/0207036](#)
13. A. Greljo, G. Isidori, D. Marzocca, JHEP **1507**, 142 (2015). [arXiv:1506.01705](#)
14. L. Calibbi, A. Crivellin, T. Ota, Phys. Rev. Lett. **115**(18), 181801 (2015). [arXiv:1506.02661](#)
15. M. Bauer, M. Neubert, [arXiv:1511.01900](#)
16. S. Fajfer, N. Kosnik, [arXiv:1511.06024](#)
17. A. Datta, M. Duraisamy, D. Ghosh, Phys. Rev. D **89**(7), 071501 (2014). [arXiv:1310.1937](#)
18. G. Hiller, M. Schmaltz, Phys. Rev. D **90**, 054014 (2014). [arXiv:1408.1627](#)
19. B. Gripaios, M. Nardecchia, S.A. Renner, JHEP **1505**, 006 (2015). [arXiv:1412.1791](#)
20. S. Sahoo, R. Mohanta, Phys. Rev. D **91**(9), 094019 (2015). [arXiv:1501.05193](#)
21. D. Becirevic, S. Fajfer, N. Kosnik, Phys. Rev. D **92**(1), 014016 (2015). [arXiv:1503.09024](#)
22. M. Freytsis, Z. Ligeti, J.T. Ruderman, Phys. Rev. D **92**(5), 054018 (2015). [arXiv:1506.08896](#)
23. B. Bhattacharya, A. Datta, D. London, S. Shivashankara, Phys. Lett. B **742**, 370 (2015). [arXiv:1412.7164](#)
24. R. Alonso, B. Grinstein, J.M. Camalich, JHEP **1510**, 184 (2015). [arXiv:1505.05164](#)
25. R. Barbieri, D. Buttazzo, F. Sala, D.M. Straub, JHEP **1207**, 181 (2012). [arXiv:1203.4218](#)
26. G. Blankenburg, G. Isidori, J. Jones-Perez, Eur. Phys. J. C **72**, 2126 (2012). [arXiv:1204.0688](#)
27. K.A. Olive et al., Particle Data Group Collaboration. Chin. Phys. C **38**, 090001 (2014)
28. G. Altarelli, R. Barbieri, Phys. Lett. B **253**, 161 (1991)
29. G. Altarelli, R. Barbieri, S. Jadach, Nucl. Phys. B **369**, 3 (1992) (Nucl. Phys. B, 376, 444, 1992)
30. R. Barbieri, M. Frigeni, F. Caravaglios, Phys. Lett. B **279**, 169 (1992)
31. V. Khachatryan et al., [CMS Collaboration], [arXiv:1509.03744](#)
32. G. Aad et al., [ATLAS Collaboration], [arXiv:1508.04735](#)